

TABLE I. Experimental parameters for the data presented in Figs. 2, 3(a), and 3(b).

Target	Laser parameters	Crystal; $2d$ (Å)	Spectral range $\Delta\lambda_R$ (Å)	Spectral resolution $\lambda/\Delta\lambda_r$	Time resolution (ps)
Fig. 2 Plane 0.2 μm Al on glass	15 J 1 beam 100 ps	TIAP 25.75	1.1	600	100
Fig. 3(a) Glass microballoon $r = 52 \mu\text{m}$ $\Delta r = 0.64 \mu\text{m}$ Coating 0.02 μm Al Gas fill 10 bar Ar	45 J (total) 2 beams 100 ps	PET 8.74	0.3	1400	70
Fig. 3(b) Glass microballoon $r = 93 \mu\text{m}$ $\Delta r = 0.56 \mu\text{m}$ Coating 0.04 μm Al Gas fill 0.5 bar Ne	45 J (total) 2 beams 100 ps	TIAP 25.75	1.8	500	70

here.

Figure 2(a) shows a streaked spectrum obtained from a plane aluminum target including the Al XII $1^1S_0-2^1P_1$ resonance line and its associated dielectronic satellites and intercombination line $1^1S_0-2^3P_1$. The dielectronic satellites are emit-

ted only during the 100-ps laser pulse and thus behave similarly to continuum emission. The resonance and intercombination line intensities decay slowly and are observable for about 600 ps. This temporal behavior is consistent with the markedly different spatial extent over which

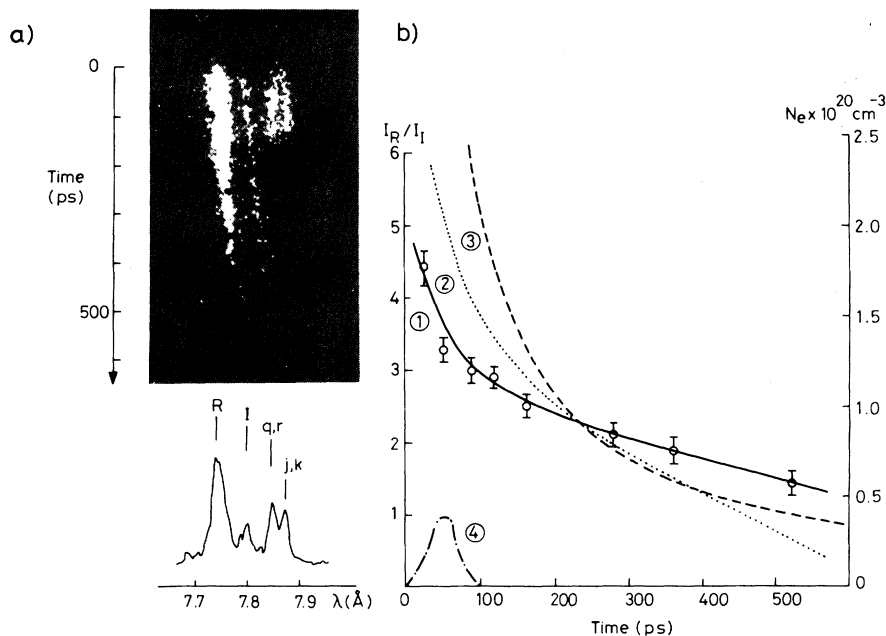


FIG. 2. (a) Streaked spectrum from a plane aluminum target with a densitometer trace at $t = 50$ ps showing the Al XII $1^1S_0-2^1P_1$ resonance line (R), its associated dielectronic satellites (q, r, j, k), and the $1^1S_0-2^3P_1$ intercombination line (I), recorded with a gold photocathode. (b) Experimental and calculated data showing the time variation of (1) the measured intensity ratio I_R/I_I of resonance-to-intercombination line, (2) the electron density N_e from (1) above, (3) N_e for self-similar planar expansion fitted at $t = 250$ ps, and (4) the laser pulse.

these lines have been observed in space-resolved spectra.^{8,9} These observations may be explained by the rapid adiabatic cooling of the plasma after the pulse. The satellite-to-resonance line-intensity ratio I_S/I_R falls with decreasing temperature¹⁰ while the resonance-to-intercombination line-intensity ratio I_R/I_I falls with decreasing density,^{1,11} and this latter effect is used here to estimate the time-varying volume-averaged electron density, N_e . Figure 2(b) shows the measured ratio I_R/I_I as a function of time and also N_e calculated for the electron temperature of 400 eV (measured by x-ray spectrometry⁸). Figure 2(b) also shows a plot of N_e for a self-similar planar expansion fitted to the experimental data at $t=250$ ps with a simple model of the form $N_e t = \text{constant}$. Discrepancies at early times may be explained by self-absorption of the resonance line¹¹ and at later times by supercooling in the plasma⁹ and a departure into nonplanar expansion.

Figure 3(a) shows a streaked spectrum obtained from an aluminum-coated glass microballoon. A simultaneously space-resolved and time-integrated spectrum showed only weak emission from the implosion core⁴; the prominent Si XIII $1^1S_0-3^1P_1$ emission is therefore mainly from the surface ablation plasma. The linewidth varies in time and reaches a maximum of 18 mÅ well resolved by the instrumental width of 4 mÅ. Line profile analysis^{4,8} indicates a peak plasma electron number density $(0.7-1.4) \times 10^{22} \text{ cm}^{-3}$. The line emission lasts for 400 ps which is significantly longer than the duration of the underlying continuum emission. The latter is about as long as the laser pulse (100 ps). The longer duration of the line emission is in the form of an afterglow during which the linewidth narrows to about the instrumental limit. The intensity decay is more rapid than for the analogous Al XII $1^1S_0-2^1P_1$ line from the plane Al target discussed above. This is due to more rapid plasma expansion from the spherical target. Time variation of resonance line shapes in afterglow emission, affects time-integrated line shapes and should be considered in spectral analysis.

A streaked spectrum from the implosion of a neon-filled microballoon (see Table I) is shown in Fig. 3(b). The Na XI $L\alpha$ line is emitted from the surface ablation plasma while the Ne X $L\beta$ line emanates from the implosion core.⁴ There is a delay of 120 ps, associated with the implosion time,⁷ between the Na XI and Ne X emission. The emission of Ne X $L\beta$ is accompanied by emission of the Ne X continuum seen beyond the continuum

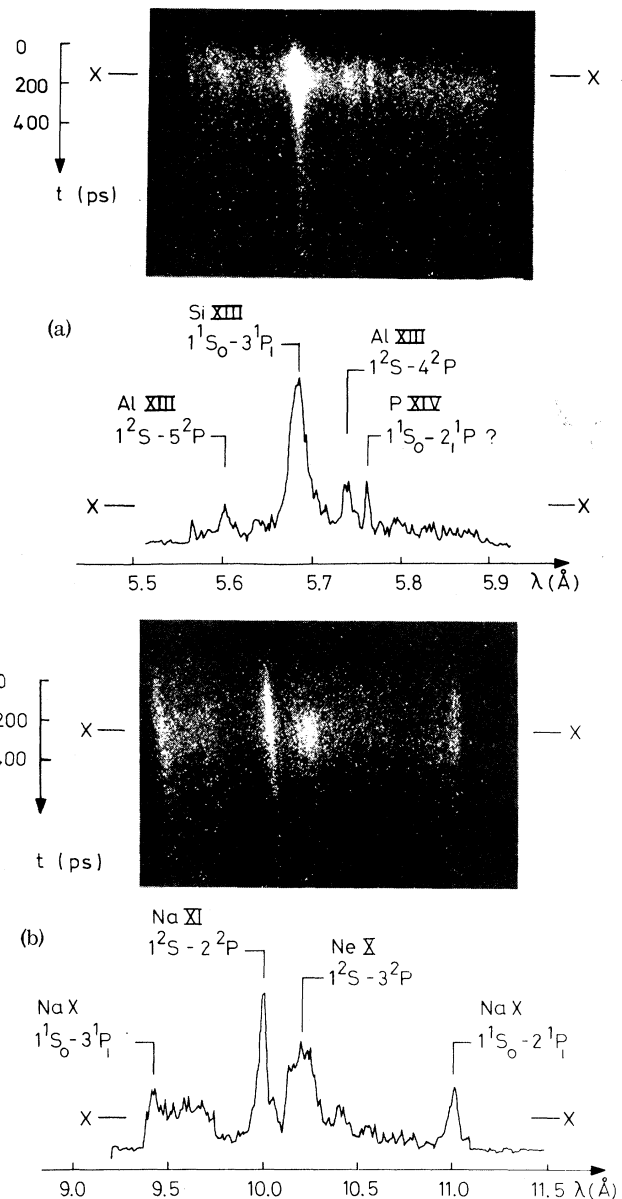


FIG. 3. (a) Streaked spectrum from an aluminum-coated glass microballoon with a densitometer trace along XX, (b) streaked spectrum from a neon-filled glass microballoon with a densitometer trace along XX, recorded with a low-density CsI photocathode.

edge in the spectrum. The Ne X $L\beta$ line persists for 200 ps and is strongly broadened with a peak linewidth of 180 mÅ greatly exceeding the 20 mÅ instrumental width; electron number density of 0.6 to $1.1 \times 10^{23} \text{ cm}^{-3}$ is indicated from analysis of the linewidth.^{4,8} The line intensity is reduced by a factor of 2 at 80 ps before and after its emission peak and the linewidth by a factor of 1.5. These changes imply a reduction of average den-

sity by a factor of 2 in this-time interval.

In conclusion, we have demonstrated the recording of transient x-ray line intensities and line shapes from laser-produced plasmas. Observations of this type have considerable potential for (a) verifying or correcting conclusions based on line shapes and intensity ratios in time-integrated spectra and (b) providing time scales for such topically interesting processes as implosion of microballoons, burn through by ablation of layers of material where the layers are identifiable by spectrally adjacent characteristic x-ray lines,⁸ and mixing through hydrodynamic instabilities in similarly identifiable layers in ablatively imploded laser fusion targets.

It is a pleasure to acknowledge the contribution of E. Bateman in developing the more sensitive low-density CsI x-ray photocathode. This work was supported by the Science Research Council.

^(a)Present address: Science Research Council Rutherford and Appleton Laboratory, Chilton, Didcot, Oxon,

OX11 0QX, United Kingdom.

¹V. A. Boiko, S. A. Pikuz, and A. Ya Faenov, *J. Phys. B* **12**, 1889 (1979).

²J. M. Auerbach *et al.*, *J. Appl. Phys.* **50**, 5478 (1979).

³B. Yaakobi *et al.*, *Phys. Rev. A* **19**, 1247 (1979).

⁴M. H. Key, J. G. Lunney, J. M. Ward, R. G. Evans, and P. T. Rumsby, *J. Phys. B* **12**, L213 (1978).

⁵K. B. Mitchell, D. B. Van Huysteyn, G. M. McCall, P. Lee, and H. R. Griem, *Phys. Rev. Lett.* **42**, 232 (1979).

⁶M. H. Key, M. J. Lamb, C. L. S. Lewis, A. Moore, and R. G. Evans, *Appl. Phys. Lett.* **34**, 550 (1979).

⁷P. H. Lee and M. D. Rosen, *Phys. Rev. Lett.* **42**, 236 (1979); P. T. Attwood *et al.*, *Phys. Rev. Lett.* **37**, 499 (1976).

⁸Annual report to the Laser Facility Committee, Science Research Council Rutherford and Appleton Laboratory Report No. RL 79-036, 1979 (unpublished).

⁹V. A. Boiko, A. Yu. Chugunov, A. Ya. Faenov, S. A. Pikuz, I. Yu. Skobelev, A. Vinogradov, and E. A. Yukov, *J. Phys. B* **12**, 213 (1979).

¹⁰C. P. Bhalla, A. H. Gabriel, and L. P. Presnyakov, *Mon. Not. Roy. Astron. Soc.* **172**, 359 (1975).

¹¹J. L. Weisheit, C. B. Tarter, J. M. Schofield, and L. M. Richards, *J. Quant. Spectros. Radiat. Transfer* **16**, 559 (1976).

Compression of Polymer-Coated Laser-Fusion Targets to Ten Times Liquid DT Density

J. M. Auerbach, W. C. Mead, E. M. Campbell, D. L. Matthews, D. S. Bailey, C. W. Hatcher, L. N. Koppel, S. M. Lane, P. H. Y. Lee, K. R. Manes, G. McClellan, D. W. Phillion, R. H. Price, V. C. Rupert, V. W. Slivinsky, and C. D. Swift

Lawrence Livermore Laboratory, University of California, Livermore, California 94550

(Received 10 March 1980)

Polymer-coated glass microspheres filled with DT fuel and argon seed gas were irradiated with the SHIVA 1.06- μm laser using 4-kJ, 200-ps (full width at half maximum), Gaussian pulses. Measured light absorption, x-ray spectrum, neutron yields, and x-ray continuum images compared favorably with detailed computer simulations. Pusher neutron activation and argon line imaging diagnostics were utilized to measure fuel density. Fuel densities of 1–3 g/cm³ or 5–15 times liquid DT density were inferred.

PACS numbers: 52.50.Jm, 52.55.Pi

Recently, much laser-driven inertial-confinement-fusion (ICF) research has turned towards the next step in achieving high-gain targets: compressing DT to high density.¹ Earlier efforts concentrated on short-pulse (< 100 ps) exploding-pusher targets² which achieved high final DT temperatures (2–8 keV) but low DT densities (~ 0.2 g/cm³). However, to achieve high gain for an ICF reactor, low-isentrope, ablatively driven implosions are required to compress DT to high densities (> 200 g/cm³).

The work reported here employed thick-walled, coated microspheres, intermediate pulse lengths, and fairly high laser irradiance to operate between these two regimes. The target designed for these experiments is shown in Fig. 1. The twenty SHIVA beams were tangentially focused with p polarization. With 4 kJ incident in a 200-ps Gaussian pulse, intensities at the poles (near the beam-cluster axis) and the equator were $\sim 4 \times 10^{15}$ W/cm², while at intermediate latitudes, intensities were $\sim 2 \times 10^{16}$ W/cm².

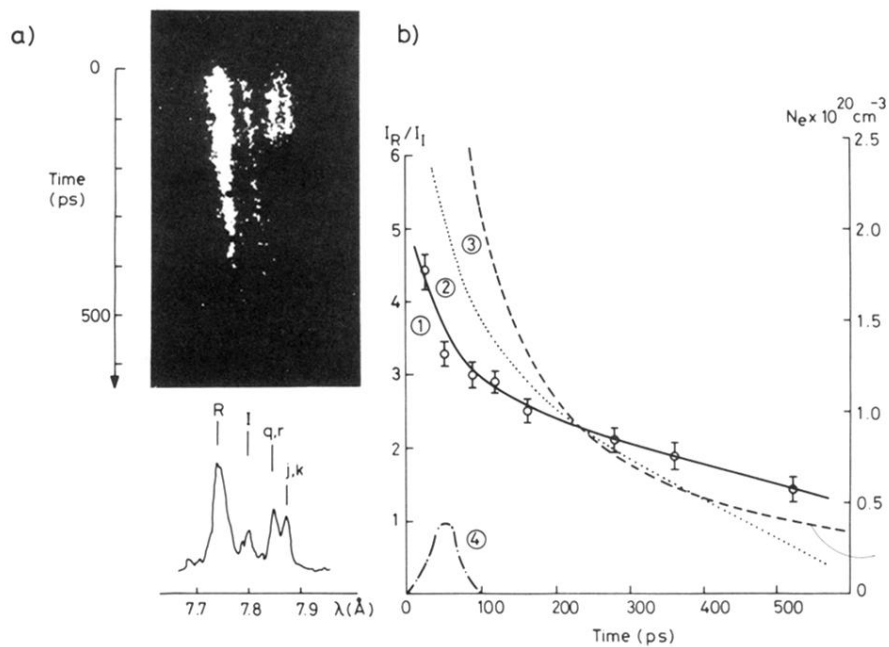


FIG. 2. (a) Streaked spectrum from a plane aluminum target with a densitometer trace at $t = 50$ ps showing the Al XII $1^1S_0-2^1P_1$ resonance line (R), its associated dielectronic satellites (q, r, j, k), and the $1^1S_0-2^3P_1$ intercombination line (I), recorded with a gold photocathode. (b) Experimental and calculated data showing the time variation of (1) the measured intensity ratio I_R/I_I of resonance-to-intercombination line, (2) the electron density N_e from (1) above, (3) N_e for self-similar planar expansion fitted at $t = 250$ ps, and (4) the laser pulse.

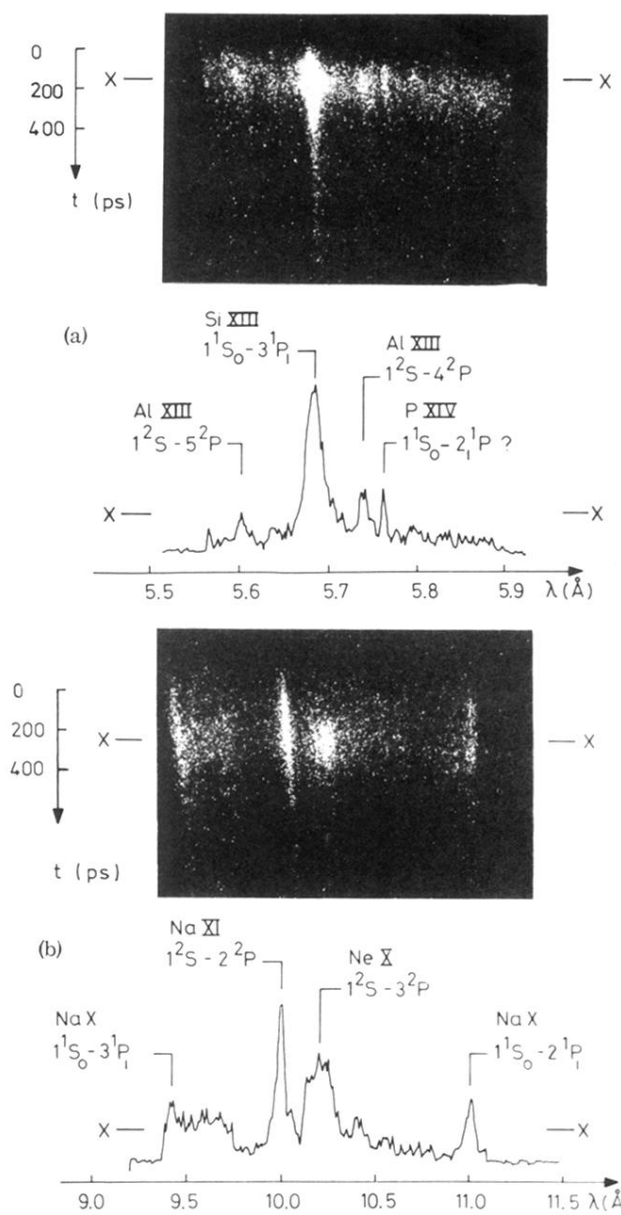


FIG. 3. (a) Streaked spectrum from an aluminum-coated glass microballoon with a densitometer trace along XX, (b) streaked spectrum from a neon-filled glass microballoon with a densitometer trace along XX, recorded with a low-density CsI photocathode.